Chemisorption of CO at Strongly Basic Sites of MgO Solid: A Theoretical Study

Xin Lu,* Xin Xu, Nanqin Wang, and Qianer Zhang

State Key Laboratory for Physical Chemistry of Solid Surfaces, Institute of Physical Chemistry, Department of Chemistry, Xiamen University, Xiamen 361005, China

Received: April 18, 2000; In Final Form: July 7, 2000

The hybrid B3LYP density functional method together with cluster models have been used to explore the adsorption and adsorption-induced dimerization and trimerization of CO over the low-coordinated oxygen anions of MgO solid. The calculations reveal the following: (i) monomeric, dimeric, and trimeric adsorptions on the low-coordinated anions lead to the formation of anionic surface species $C_mO_{m+1}^{2-}$ ($m = 1-3$); (ii) dioxoketene ion $C_2O_3^{2-}$ which has a strong C═C bond can be formed at O_{3C} site, whereas at O_{4C} site the formation of triplet *trans*-$C_2O_3^{2-}$ adspecies is thermodynamically favorable over the formation of singlet $C_2O_3^{2-}$ adspecies which has a weak C−C bond; (iii) The $C_3O_4^{2-}$ surface species does have a ketenic group, i.e., O═C═C<, and shows substantial stability. The calculated energetics suggests that the dimeric adspecies are unlikely to be stable adspecies, but may be the intermediates for the formation of higher oligomeric adspecies of CO. The calculated IR frequencies of $C_mO_{m+1}^{2-}$ ($m = 1-3$) surface complexes have been compared with the experimental IR spectra.

1. Introduction

Owing to its important implications for heterogeneous catalysis and other surface processes, the adsorption of CO on MgO has been of continuous interest from both experimental and theoretical points of view.[1−29] CO is a most widely used probe molecule for acid site in surface science. IR experiments[1−4] revealed that CO adsorption on well-defined MgO(001) surface at low temperatures (e.g., 77 K) gives rise to C−O stretching frequencies higher than that of the free molecule (2143 cm^{-1}). This phenomenon has been well ascribed to CO weakly adsorbed on top of the acidic sites, i.e., Mg_{XC}^{2+} ($X = 3-5$).[1−11] However, on thermally activated MgO samples, CO adsorption was found to result in complex IR spectra, including those absorption bands (>2143 cm^{-1}) pertinent to CO adsorbed on Mg_{XC}^{2+} sites and ones in the range 1000−2100 cm^{-1}.[1−8] The latter are rather complicated and have been tentatively attributed to surface species formed upon CO chemisorption on the low-coordinated anions, i.e., O_{YC}^{2-} ($Y = 3,4$), that are of stronger basicity than the 5-coordinated anions. Accordingly, a variety of surface species, such as CO_2^{2-}, CO_3^{2-}, $C_2O_2^{-}$, $C_2O_2^{2-}$, $C_2O_3^{2-}$, $C_3O_4^{2-}$, and $C_mO_{m+2}^{4-}$ or $(CO)_m^{2-}$ ($m > 4$), have been postulated so far on the basis of the results of IR, UV, EPR, and TPD experiments.[5−8,13−15] Meanwhile, several reaction pathways, such as disproportionation and/or oligomerization of CO, were put forward to account for the formation of those surface species on MgO solid.[5−8,13−15] Despite the continuous efforts that have been paid on this subject from early 1970s, no unambiguous assignment of the complex IR spectra has been accomplished yet, providing an interesting and challenging problem to both experimentalists and theoreticians.

Since the early 1980s, intensive attention from theoreticians has been paid to the CO/MgO adsorption system,[16−28] from the earliest ab initio study of Colbourn[16] to the very recent periodic DFT (density functional theory) study of Synder et al.,[23] mainly focusing on the nature of the bonding between CO and acid sites and on the nature of the adsorption-induced blue-shift of CO stretching mode frequency. Only a few of them can be related to CO chemisorption onto the strongly basic sites (O_{3C}^{2-} and O_{4C}^{2-}).[25−28] Matsumura et al. investigated at the SCF level the trapping and oxidation of CO at surface step sites of MgO solid using a $(MgO)_3$ cluster embedded with 84 point ions of $\pm 0.18e$, and predicted that CO oxidation could be caused by removing a low-coordination oxygen ion from the step sites.[25] Huzimura et al. studied the O-isotope exchange between adsorbed CO and MgO surfaces using an ab initio MO method.[26] A site with a combination of an oxygen vacancy and low-coordinated oxygen atoms has been suggested to account for the O-exchange reaction.[26] Ab initio calculations by Klabunde et al. revealed that the interaction of CO with MgO and CaO molecules results in complexes containing a metal dication coordinated to a bent CO_2^{2-} ligand.[27] Using density functional method, Kobayashi et al. examined the interaction of CO molecule with MgO surfaces and the possible mechanisms for the adsorbed and gas-phase CO exchange reaction.[28] They predicted that adsorption of CO to the surface O atom is unstable, but becomes stable only when the adjacent Mg site is occupied by another CO molecule. A larger contribution of the ionic bonding for the CO−surface O atom bonding was predicted in their calculations.[28] This theoretical prediction seems in contradiction to the experimental inference that CO can be bonded covalently onto the low-coordinated anions, forming CO_2^{2-} surface species.[5−8,13−15]

In the present work, the bonding of CO to the basic, low-coordinated anions (O_{3C}^{2-} and O_{4C}^{2-}) on MgO solid and the possibility of its dimer and trimer formation over those surface sites have been investigated by means of first-principles density functional cluster model calculations. The vibrational frequencies of the so-formed $C_mO_{m+1}^{2-}$ ($m = 1-3$) surface species have been calculated and compared with the available experimental IR spectra of CO/MgO chemisorption system. To the best of our knowledge, this is the first electronic structure study

* Corresponding author. Fax: +86-592-2183047. E-mail: xinlu@xmu.edu.cn.

10.1021/jp0014622 CCC: $19.00
Published on Web 10/04/2000

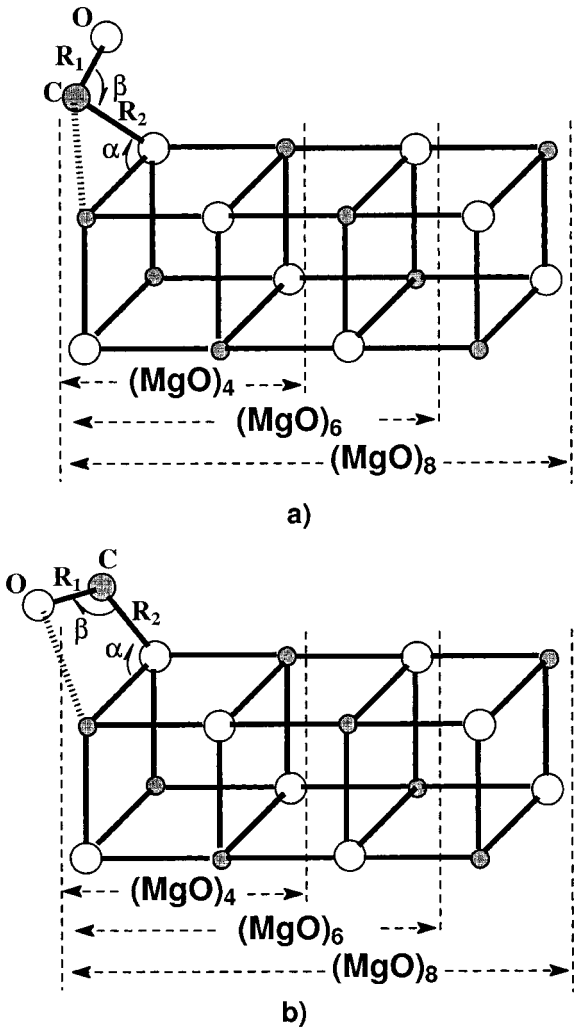

Figure 1. Configurations of CO adsorbed on the $O_{3C}-Mg_{3C}$ pair site: (a) bridge mode and (b) chain mode.

regarding the adsorption-induced dimerization and trimerization of CO over metal oxides. It should be mentioned that dimerization and trimerization of CO were also supposed to occur on other alkaline-earth metal oxides and rare-earth metal oxides, e.g., CaO, SrO, and La_2O_3.[29]

2. Computational Details

Solid MgO has a rocksalt structure with its nearest Mg−O distance being 2.104 Å.[30] It has been believed that edges and corners, where the low-coordinated Mg and O atoms are located, are abundant and characteristic features of thermally activated MgO microcrystals.[15] In our calculations, we have used three neutral $(MgO)_n$ (n = 4,6,8) clusters (See Figure 1). The 3- or 4-coordinated Mg and O atoms are denoted as Mg_{3C}, O_{3C}, Mg_{4C}, and O_{4C}, respectively. As such, there are several types of low-coordinated O−Mg pairs existing in the $(MgO)_n$ (n = 4, 6, 8) clusters, namely, $O_{3C}-Mg_{3C}$, $O_{3C}-Mg_{4C}$, $O_{4C}-Mg_{3C}$, and $O_{4C}-Mg_{4C}$, which would be the models of possible surface active sites available at the steps, kinks, and corners of MgO solid.

In principle, slab models or large, embedded clusters are superior to the finite, bared cluster models in the modeling of an extended metal oxide surface. It is clear that one must be extremely cautious when attempting to model the chemistry of the extended metal oxide surfaces using a finite cluster.[31,32] "Small cluster models may nevertheless be useful for rapidly identifying possible trends, binding modes, and reactions, and for gaining qualitative insights into behaviors on nonideal surfaces."[33] Indeed, the above-chosen $(MgO)_n$ (n = 4,6,8) cluster models in conjunction with the hybrid density functional B3LYP method[34,35] were successfully employed to investigate N_2O decomposition,[36] NO adsorption,[37,38] C_2H_2 adsorption,[39] and O adsorption[32] on low-coordinated sites of MgO solid as well as CO adsorption on low-coordinated acidic sites of MgO solid.[21] Similar cluster models were also adopted in the theoretical studies of CO adsorption[28] and the dissociative adsorption of H_2[40] on the low-coordinated sites of MgO solid.

For all calculations throughout, we used the hybrid ab initio density functional B3LYP method, which includes a three-parameter hybrid density functional that combines the gradient-corrected exchange functional of Becke and the correlation functional of Lee, Yang, and Parr with the Hartree−Fock exchange.[34,35] As mentioned above, this hybrid DFT method has been proven to give reasonable prediction of the adsorbate structures and adsorption energies in the studies of small molecules on MgO solid.[21,36−40] It seems that some pure density functional methods without including gradient correction, e.g., the local density approximation (LDA), would possibly overestimate the CO binding energy, as shown by Neyman et al. in their DFT study of CO adsorption on the acidic sites of MgO-(100) surface.[19]

The basis sets used in the present study are the standard 6-31+G* basis sets[41] for O and C, and 6-31G* basis set[41] for Mg. For free CO molecule, the calculated C−O bond length is 1.139 Å, in good agreement with the experimental value of 1.131 Å.[42] The geometries of adsorbed species were optimized in internal coordinates with all the substrate atoms being fixed at the bulk values. Unless otherwise specified, the adsorption properties were obtained without relaxation of the adsorptive sites. Optimizations have been done by using Berny algorithm with *Gaussian94*.[41]

3. Monomeric Adsorption of CO

CO on $Mg_{3C}-O_{3C}$ Pair Site. For CO adsorption at $Mg_{3C}-O_{3C}$ site on the $(MgO)_n$ (n = 4,6,8) clusters, two local minima were located and depicted in Figure 1a,b. One is a bridge mode, i.e., CO bridges over the $Mg_{3C}O_{3C}$ ion pair with its C-end down (see Figure 1a). Another is a chain mode, i.e., CO lies over the $O_{3C}-Mg_{3C}$ ion pair (see Figure 1b). The calculated geometric parameters and binding energies for CO adsorbed in the two modes are given in Table 1.

In both adsorption modes, the intermolecular $C-O_{3C}$ distances range within 1.45−1.50 Å, implying the formation of a covalent bond between CO and O_{3C}. The intermolecular $C-Mg_{3C}$ distances are about 2.13 Å in the bridge mode. The intramolecular C−O bond length of CO molecule is elongated substantially (>0.06 Å) upon adsorption, and the extent of C−O bond elongation is more severe for the chain mode adsorption. This implies that both modes of adsorption induce substantial activation of the intramolecular C−O bond, but in the bridge mode the adsorbed CO is less activated. In accordance with the above results, Mulliken population analysis and NBO (natural bond orbital)[43] analysis reveal the following: (i) for both modes of adsorption, a much localized bond is formed between the lone pair on O_{3C} and the empty $2\pi^*$ MO (molecular orbital) of the CO; (ii) for the bridge mode adsorption, there exists a slight electron transfer from the CO 5σ MO to the empty atomic orbitals on Mg_{3C}. Consequently, (iii) CO adsorbed is considerably charged with a natural charge of −0.46 in the chain mode and of −0.34 in the bridge mode, respectively; (iv) the

TABLE 1: Geometrical Parameters,[a] Binding Energies[b] (kcal/mol) for CO Adsorption on $O_{YC}-Mg_{XC}$ ($X,Y = 3,4$) Sites

ads. site	cluster model	ads. mode	sym.[c]	R_1 (Å)	R_2 (Å)	α (°)	β (°)	Q(CO)NC	Q(COO_{XC}) NC	E_b
$O_{3C}-Mg_{3C}$										
	$(MgO)_4$	chain	C_S	1.260	1.454	89.0	108.2	−0.46	−1.74	−16.3
		chain[d]	C_S	1.267	1.421	83.4	110.7	−0.49	−1.78	−19.0
		bridge	C_S	1.197	1.478	70.8	119.4	−0.34	−1.62	−16.4
	$(MgO)_6$	chain	C_1	1.262	1.459	88.8	108.0	−0.46	−1.75	−16.7
		bridge	C_1	1.195	1.501	70.0	118.6	−0.34	−1.63	−16.2
	$(MgO)_8$	chain	C_1	1.263	1.458	88.8	108.0	−0.46	−1.74	−15.9
		bridge	C_1	1.196	1.496	70.2	118.8	−0.34	−1.63	−15.3
$O_{3C}-Mg_{4C}$										
	$(MgO)_6$	chain	C_S	1.238	1.503	91.2	106.7	−0.40	−1.73	−4.6
		bridge	C_S	1.143	2.361	63.9	165.1	−0.07		−7.4
	$(MgO)_8$	chain	C_S	1.240	1.501	91.1	106.7	−0.41	−1.73	−4.0
		bridge	C_S	1.144	2.345	63.7	165.7	−0.09		−7.0
$O_{4C}-Mg_{3C}$										
	$(MgO)_6$	chain	C_S	1.252	1.392	94.7	110.3	−0.47	−1.71	−19.5
		chain[d]	C_S	1.253	1.392	93.5	110.5	−0.49	−1.73	−18.7
		bridge	C_S	1.139	2.275	71.0	164.2	−0.07		−10.7
	$(MgO)_8$	chain	C_S	1.254	1.424	91.5	109.2	−0.47	−1.74	−12.3
		bridge	C_S	1.138	2.277	71.5	164.5	−0.07		−10.0
$O_{4C}-Mg_{4C}$										
	$(MgO)_8$	chain	C_S	1.220	1.444	105.8	112.6	−0.41	−1.69	−10.2
		bridge	C_S	1.139	2.398	71.1	163.5	−0.03		−4.8

[a] For the nomenclature of the geometric parameters in this table, please refer to Figures 1−4. [b] Binding energy $E_b = E[CO/(MgO)_n] - E(CO) - E[(MgO)_n]$. [c] In those systems of C_1 symmetry, the optimized dihydral angle between the C−O−Mg_{3C}-O_{3C} plane and the substrate surface is nearly 135°. [d] The O_{YC} site is allowed to relax.

TABLE 2: Geometrical Parameters[a] and Dissociation Energies[b] for $C_2O_3^{2-}$ Species Formed on O_{YC} ($Y = 3,4$) Sites

cluster	site	spin state	mode	sym.	R_1 (Å)	R_2 (Å)	R_3 (Å)	R_4 (Å)	α (°)	β (°)	γ (°)	δ (°)	D_e (kcal/mol) CO	D_e (kcal/mol) 2CO
$(MgO)_4$	O_{3C}													
		1		C_1[c]	1.425	1.332	1.325	1.196	84.5	113.2	128.9	178.9	1.4	18.1
		3	tran	C_S	1.404	1.296	1.415	1.227	86.3	113.0	127.8	127.7	−4.1	12.6
		3[d]	trans	C_S	1.397	1.301	1.418	1.225	80.3	115.1	125.5	128.4	−3.7	15.3
		3	cis	C_S	1.397	1.300	1.415	1.221	86.5	112.9	129.0	130.7	−6.2	10.5
$(MgO)_6$	O_{4C}													
		1		C_1[c]	1.406	1.229	1.736	1.245	83.3	116.5	17.6	108.1	−0.3	19.2
		3	trans	C_S	1.429	1.273	1.414	1.254	81.9	116.8	123.4	128.3	4.8	24.3
		3[d]	trans	C_S	1.386	1.274	1.418	1.258	84.4	116.3	124.5	128.9	11.5	30.2
		3	cis	C_S	1.391	1.275	1.425	1.222	85.2	116.1	129.4	133.5	−2.4	17.1
$(MgO)_8$	O_{4C}													
		1		C_1[c]	1.432	1.224	1.723	1.246	84.5	115.8	118.2	109.0	−2.8	7.4
		3	trans	C_S	1.441	1.257	1.414	1.257	83.2	116.0	124.2	129.3	0.5	10.7
		3	cis	C_S	1.403	1.259	1.429	1.225	86.9	115.9	129.7	132.8	−6.0	4.2

[a] For the nomenclature of the geometric parameters in this table, please refer to Figure 5. [b] $D_e(CO) = E[CO/(MgO)_n] + E(CO) - E[2CO/(MgO)_n]$; $D_e(2CO) = E[(MgO)_n] + 2E(CO) - E[2CO/(MgO)_n]$. [c] The so-formed $C_2O_3^{2-}$ species is nearly planar. [d] The O_{YC} site is allowed to relax.

total natural charge on the (CO + O_{3C}) group is −1.74 and −1.63 for the chain and bridge modes, respectively. The (CO + O_{3C}) group, hence, could be regarded as dioxocarbene CO_2^{2-}. The calculated binding energies for the two modes of CO adsorption are comparable, centering around 16 kcal/mol. Moreover, it is noteworthy that for the adsorption of CO in the bridge mode (or in the chain mode) over the $O_{3C}-Mg_{3C}$ pair site on the three $(MgO)_n$ ($n = 4, 6, 8$) clusters of different size, the calculated adsorption properties, including geometrical parameters and binding energies, show negligible dependence on the cluster size. A similar trend of size-independence was also obtained in our previous quantum chemical studies of the O/$(MgO)_n$ and NO/$(MgO)_n$ ($n = 4,6,8$) model systems.[32,37]

CO on $Mg_{4C}-O_{3C}$, $Mg_{3C}-O_{4C}$, and $Mg_{4C}-O_{4C}$ Pair Sites. Similar to CO adsorption on the $Mg_{3C}-O_{3C}$ site, two adsorption modes, i.e., a bridge mode and chain mode, have been found for CO adsorptions over the $Mg_{4C}-O_{3C}$, $Mg_{3C}-O_{4C}$, and $Mg_{4C}-O_{4C}$ ion pairs on the $(MgO)_6$ and $(MgO)_8$ clusters. The adsorption configurations are depicted in Figures 2a,b, 3a,b, and 4a,b, separately. The optimized geometric parameters and binding energies are included in Table 1.

For the chain mode adsorption over these ion pairs, detailed wave function analysis indicates that the bonding mechanism is similar to that of the chain mode adsorption over the $Mg_{3C}-O_{3C}$ site. The bonding between CO and O_{YC} ($Y = 3,4$) involves a covalent, dative bond between the lone pair on O_{4C} atom and the $2\pi^*$ MO of CO. This results in a substantial net charge (>0.40e) on the admolecule along with an intramolecular C−O bond elongation (∼0.12 Å) upon adsorption in chain mode. The short intermolecular C−O_{YC} distance (1.39−1.50 Å) and the negative charge (∼−1.70) on the (CO + O_{YC}) group strongly suggests it is CO_2^{2-}-like.

In the bridge mode, both the C−Mg_{XC} (see R_2 in Table 2) and O−O_{YC} distances are too long (>2.2 Å); the net charge on the admolecule is trivial ($Q_{CO} < 0.1e$); the calculated binding energy ranges within −4.8 to −10.7 kcal/mol. As such, CO is physisorbed over these pair sites. This is different from the bridge mode adsorption over the $Mg_{3C}-O_{3C}$ pair site, by which a covalent dative bond can be formed between O_{3C} surface anion and CO, but similar to the bridge mode adsorption of NO over the $Mg_{XC}-O_{YC}$ ($X,Y = 3,4$) pair site on MgO solid.[37,44] Such kind of bridge-mode adsorption of CO on low-coordinated pair

sites of MgO solid was also predicted by Kobayashi et al. in their DFT cluster model study,[28] despite the fact that their predicted adsorption energies are substantially higher than those predicted in the present work. Nevertheless, the calculated adsorption properties given in Table 1 show that monomeric adsorption of CO on the low-coordinated $Mg_{XC}-O_{YC}$ (X,Y = 3,4) pair sites is site-dependent.

4. Dimeric Adsorption of CO

In our previous theoretical study regarding NO adsorption on MgO solid, we found that NO can be adsorbed dimerically onto the low-coordinated anions (O_{YC}^{2-}(Y = 3,4)), producing $N_2O_3^{2-}$ surface species.[37,44] The $N_2O_3^{2-}$ moiety was found to be closed-shell with a σ-bond and a π-bond forming between the two N atoms of the NO_2^{2-} species and of the in-coming NO. Analogously, one may expect the formation of $C_2O_3^{2-}$ species upon attaching another CO onto the CO_2^{2-} adspecies in the CO/MgO chemisorption system. The $C_2O_3^{2-}$ adspecies, if it exists, would has two fewer valence electrons than has the $N_2O_3^{2-}$ adspecies, and can be either in singlet (closed-shell) or in triplet (open-shell). The formation of triplet $C_2O_3^{2-}$ from singlet CO_2^{2-} and CO is, however, spin-forbidden. Singlet $C_2O_3^{2-}$ moiety may exist in a ketenic form (O=C=C<), i.e., dioxoketene ion, as suggested by some experimentalists.[7] The possibility of the formation of both singlet and triplet $C_2O_3^{2-}$ species has been considered in our calculations. The optimized geometric parameters and calculated dissociation energies of the singlet and triplet $C_2O_3^{2-}$ species formed on $(MgO)_n$ (n = 4,6,8) are presented in Table 2, the corresponding adsorption configurations are depicted in Figure 5.

For the singlet $C_2O_3^{2-}$ moiety (Figure 5a) formed at the O_{3C} of $(MgO)_4$ cluster model, the optimal C−C bond length is around 1.32 Å, which is typical of C=C double bond; the C−O bond length in the second CO molecule is only 1.196 Å; the C−C−O bond angle (δ) is 178.9°. These structural features demonstrate the presence of a ketenic group (O=C=C<) in the singlet $C_2O_3^{2-}$ moiety. Hence, the singlet $C_2O_3^{2-}$ moiety formed at the O_{3C} site is indeed a dioxoketene ion. For the singlet $C_2O_3^{2-}$ moiety formed at the O_{4C} site on $(MgO)_n$ (n = 6,8) cluster model, we found rather different structural features. Surprisingly, the C−C bond length is around 1.73 Å, even longer than the typical C−C single bond length (∼1.56 Å); the C−C−O bond angle bends severely to ∼109°, probably due to the electrostatic attraction of the nearest surface Mg cation. Therefore, the singlet $C_2O_3^{2-}$ moiety formed at the O_{4C} site cannot be a dioxoketene ion. Indeed, Mulliken population analysis and NBO analysis reveal a moderate dative bond between the lone pair at the C atom of the CO_2^{2-} moiety and the empty $2\pi^*$ MO of the second CO.

So far as the energetics of the singlet $C_2O_3^{2-}$ formation has been considered, it can be seen from Table 2 that the attachment of a second CO onto the CO_2^{2-} moiety is slightly exothermic (by 1.4 kcal/mol) at the O_{3C} site, but slightly endothermic (by 0.3 and 2.8 kcal/mol) at the O_{4C} site (on $(MgO)_6$ and $(MgO)_8$ cluster models). It seems that the formation of a singlet $C_2O_3^{2-}$ is thermodynamically favorable at the O_{3C} site, but unfavorable at the O_{4C} site. We suspect that the singlet $C_2O_3^{2-}$ at O_{4C} site, if exists, may be an intermediate leading to the formation of higher oligomeric adspecies, e.g. $C_3O_4^{2-}$.

For triplet $C_2O_3^{2-}$ species, we have found two conformers (Figure 5b,c), which have the same topological structures as the *trans*- and *cis*-$N_2O_3^{2-}$ species that were previously found in the NO/MgO system.[37,44] Accordingly, they are denoted as *trans*-$C_2O_3^{2-}$ (Figure 5b) and *cis*-$C_2O_3^{2-}$ (Figure 5c), respectively. The optimal C−C bond length is around 1.43 Å; the C−O bond lengths fall into two groups, i.e., the C−O_{YC} (Y = 3,4) bond length (R_1) is around 1.40 Å, the other two C−O bonds (R_2 and R_4) around 1.25 Å. It is thus deducible that in the triplet $C_2O_3^{2-}$, the bond order of the C−C bond is probably 1.5, and the C−O_{YC} bonding is covalent, but weaker than the two C−O bonds in the in-coming $(CO)_2$. The natural charge on the triplet C_2O_3 moiety is around −1.75; the spin density is mainly localized at the two in-coming CO molecules. The calculated energetics given in Table 2 indicate the following: (i) the trans- form is always more stable than the cis- form; (ii) among those triplet $C_2O_3^{2-}$ species concerned, the *trans*-$C_2O_3^{2-}$ formed at the O_{4C}^{2-} site is the most stable. It is, however, notable that with respect to CO_2^{2-} species and free CO molecule, the formation of triplet $C_2O_3^{2-}$ species is not energetically favorable, except the formation of *trans*-$C_2O_3^{2-}$ at the O_{4C}^{2-} site. The calculated formation energies suggest that triplet $C_2O_3^{2-}$ species, if it exists, is intermediate-like. Furthermore, its biradical feature suggests it could be ESR-detectable. Indeed, Klabunde et al. detected a variety of adspecies in the CO/MgO and CO/CaO chemisorption systems using ESR technique.[13,14] They assigned those ESR-active adspecies to the anionic radical $C_2O_2^-$, and, later on, to the rhodizonate trianion $C_6O_6^{3-}$ as well

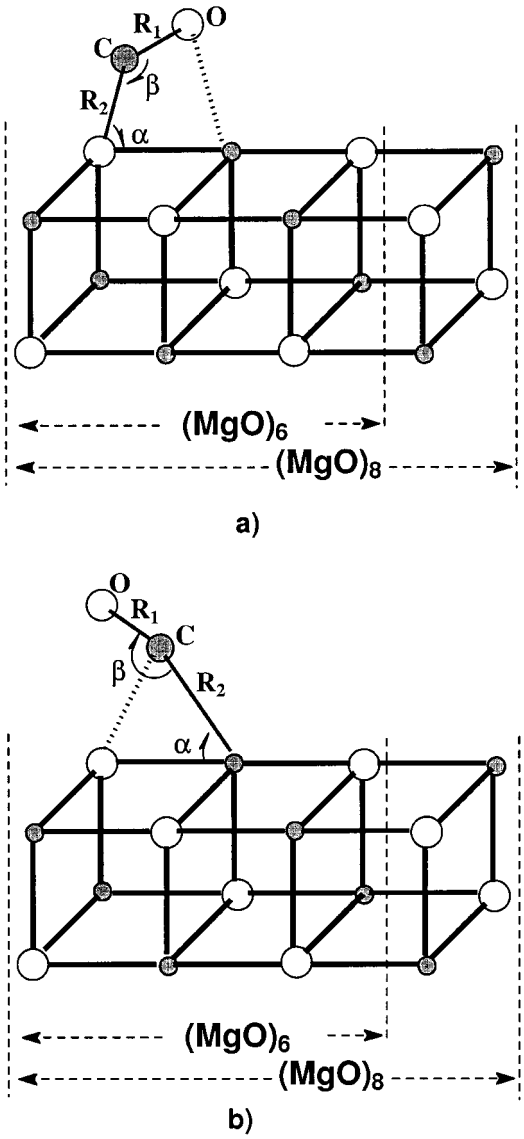

Figure 2. Configurations of CO adsorbed on the $O_{3C}-Mg_{4C}$ pair site: (a) chain mode and (b) bridge mode.

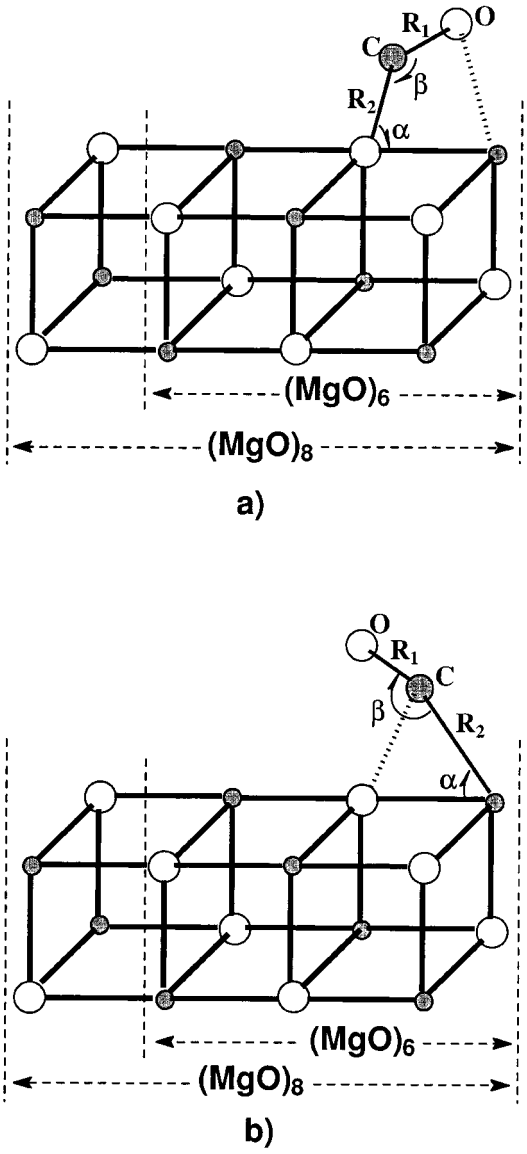

Figure 3. Configurations of CO adsorbed on the $O_{4C}-Mg_{3C}$ pair site: (a) chain mode and (b) bridge mode.

as the complex species converted from this anion by heating or by treatment with a variety of adsorbing secondary chemical reagent. Considering its bi-radical feature, we suspect that triplet $C_2O_3^{2-}$ moiety may be the very ESR-active moiety detected experimentally or a key intermediate that leads to the formation of ESR-active, higher oligomeric adspecies of CO.

We then consider the relative stability of singlet and triplet $C_2O_3^{2-}$ species. At the O_{3C} site, the singlet, ketenic $C_2O_3^{2-}$ is more stable than the triplet ones, while at the O_{4C} site the singlet $C_2O_3^{2-}$ is less stable than the triplet ones. As a direct, adiabatic formation of triplet $C_2O_3^{2-}$ from singlet CO_2^{2-} and CO is spin-forbidden, it is deducible that the formation of triplet $C_2O_3^{2-}$ should be a process photoactivated. On the other hand, we suspect that the formation of singlet $C_2O_3^{2-}$ may be a thermo-activated process. The kinetics for the formation of singlet and triplet $C_2O_3^{2-}$ will be considered in future work.

5. Trimeric Adsorption of CO

The geometry of the $C_2O_3^{2-}$ species leaves the possibility of attaching a third CO onto it to form $C_3O_4^{2-}$ surface species. To check this possibility, we performed B3LYP calculations regarding trimeric adsorption of CO over the O_{3C}^{2-} sites and

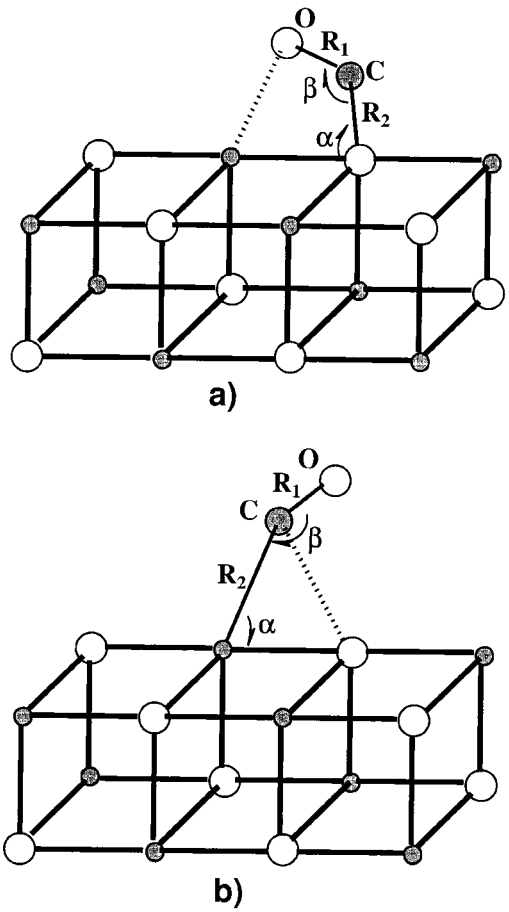

Figure 4. Configurations of CO adsorbed on the $O_{4C}-Mg_{4C}$ pair site: (a) chain mode and (b) bridge mode.

O_{4C}^{2-} sites on the $(MgO)_n$ ($n = 4,6$) cluster models, respectively. Our calculations showed that further attachment of a CO molecule onto the $C_2O_3^{2-}$ species is energetically favorable, leading to the formation of a stable $C_3O_4^{2-}$ moiety (see Figure 6). For the sake of brevity, only the properties of the trimeric adsorption at the O_4^{2-} site on $(MgO)_6$ cluster model are reported.

At the O_{4C}^{2-} site, the formation energy of the $C_3O_4^{2-}$ adspecies is 39.9 kcal/mol with respect to a free CO molecule and a *trans*-$C_2O_3^{2-}$ surface species, or 64.4 kcal/mol with respect to 3 free CO molecules and bare O_{4C} surface site. As depicted in Figure 6, the optimal bond angle ∠O3−C3−C2 is nearly 180°; the optimal bond lengths of O3−C3 and C3−C2 are 1.16 and 1.37 Å, respectively. This structural feature indicates the presence of a O═C═C< ketenic group in the $C_3O_4^{2-}$ surface species. This finding is in agreement with the revised viewpoint of Zecchina et al.[2] and the inference made by Tashiro et al.[8] However, Zecchina et al. suggested that the specific sites responsible for the formation of $C_3O_4^{2-}$ species are those corner sites, i.e., O_{3C}^{2-}. Our calculations revealed that $C_3O_4^{2-}$ species is also formable at 4-coordinate O_{4C}^{2-} sites. In the following section, we will show that the calculated vibrational frequencies of the so-formed $C_3O_4^{2-}$ are in good agreement with the experimental IR frequencies of K_3 species supposed by Zecchina et al.[2] and Tashiro et al.[8]

6. Effect of Surface Site Relaxation

At this stage, one might question what effect allowing some amount of surface relaxation has on the adsorbate structures and on the adsorption energies. Note that for all $C_mO_{m+1}^{2-}$ ($m = 1-3$) adspecies concerned, a much covalent $C-O_{YC}$

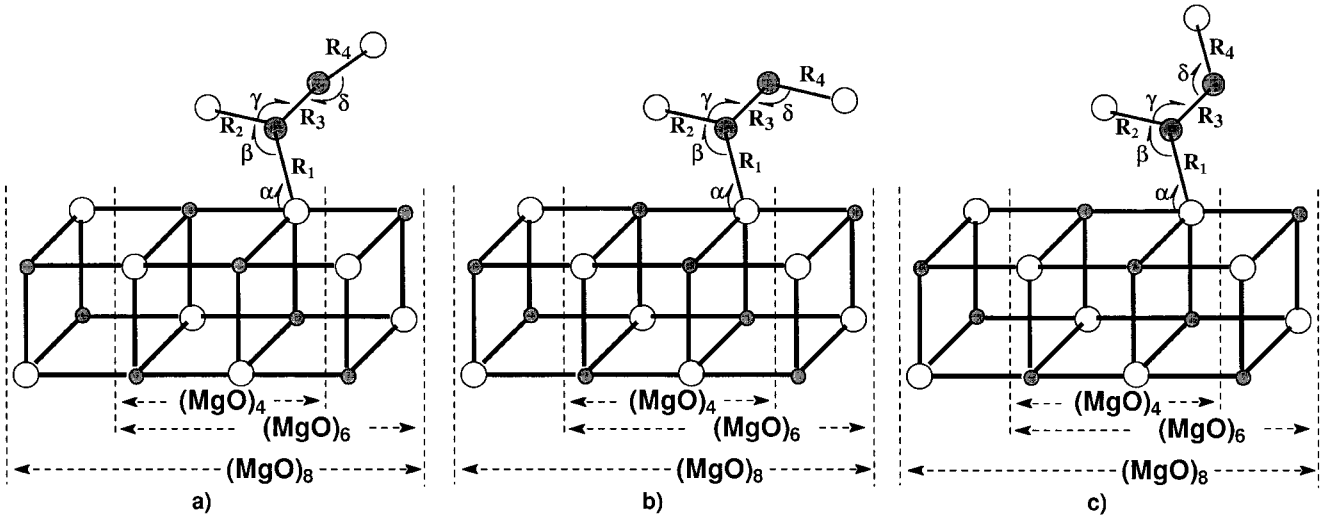

Figure 5. Three configurations of $C_2O_3^{2-}$ ion on the $(MgO)_n$ (n = 4,6,8) cluster model: (a) singlet $C_2O_3^{2-}$, (b) triplet *trans*-$C_2O_3^{2-}$, (c) triplet *cis*-$C_2O_3^{2-}$.

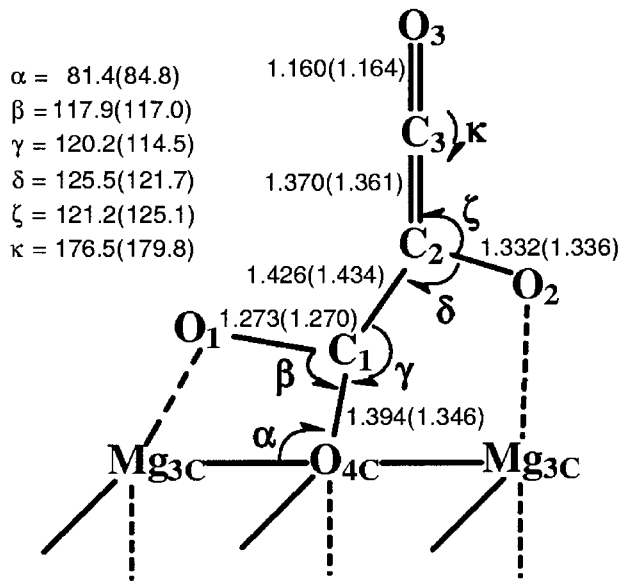

Figure 6. Configuration of $C_3O_4^{2-}$ moiety formed at the O_{4C} site of $(MgO)_6$ cluster model (the geometric parameters given in parentheses are obtained by allowing the O_{4C} site to relax).

(Y = 3,4) bond is formed between the adsorptive O_{YC} site and the incoming $(CO)_m$ species. It is deducible that the O_{YC} atom may deviate severely from its lattice site upon chemisorption. Accordingly, we take partially the surface relaxation into account by allowing the adsorptive O_{YC} site to relax in the following calculations. These are for CO_2^{2-} formed at the O_{3C} site of $(MgO)_4$ and at the O_{4C} site of $(MgO)_6$ (see Table 1 for geometries and energetics), for triplet *trans*-$C_2O_3^{2-}$ species formed at the O_{3C} site of $(MgO)_4$ and at the O_{4C} site of $(MgO)_6$, (see Table 2 for geometries and energetics) and for $C_3O_4^{2-}$ species formed at the O_{4C} site of $(MgO)_6$ (See Figure 6 for geometry).

For CO_2^{2-} species formed at the O_{3C} site, the O_{3C} site is found to deviate outward from its ideal lattice site by 0.32 Å; (before adsorption, the O_{3C} site is attracted inward from its ideal lattice site by 0.07 Å by the neighboring Mg atoms.); the distance of the forming C−O_{3C} bond is by 0.03 Å shorter than the nonrelaxed case; the deviation of the bond angles from the nonrelaxed case is within several degrees. The predicted binding energy is 19.0 kcal/mol, which is by 2.7 kcal/mol more stable than the nonrelaxed case. However, negligible difference is found between the relaxed and nonrelaxed cases for CO_2^{2-} formed at the O_{4C} site of the $(MgO)_6$ cluster.

For the triplet *trans*-$C_2O_3^{2-}$ species formed at O_{3C} site of $(MgO)_4$ and at O_{4C} site of $(MgO)_6$, the surface site relaxation shows negligible effect on the geometries of the adsorbates, but has nontrivial effect on the predicted formation energies. For both adspecies, higher formation energies (cf., Table 2) are obtained upon surface site relaxation.

For $C_3O_4^{2-}$ species formed at the O_{4C} site of $(MgO)_6$, the predicted formation energy is 72.7 kcal/mol after the relaxation of the O_{4C} site is considered. This is by 8.3 kcal/mol more exothermic than the nonrelaxed case. The optimal geometric parameters are given in parentheses in Figure 6, showing that the relaxation has trivial effect on the predicted bond lengths of $C_3O_4^{2-}$ species.

7. Vibrational Frequencies of $C_mO_{m+1}^{2-}$ (m = 1−3) Species

The calculated IR frequencies of CO_2^{2-} species formed on O_{3C}^{2-} and O_{4C}^{2-} site are given in Table 3. For free CO, the B3LYP/6-31+G*-calculated C−O stretch frequency is 2204 cm^{-1}, which is obviously overestimated with respect to the experimental value of 2143 cm^{-1}. A scale factor of 0.975 is thus employed to all the C−O stretch mode frequencies. The scaled values are also included in Table 3. In their FTIR experiments,[8] Tashiro et al. assigned the three peaks at 1475, 1315, and 1280 cm^{-1} to the C−O stretch modes of the linear monomer on low-coordinated O^{2-} sites and of the chained monomers on low-coordinated O^{2-} sites of different coordination environments, respectively. Babaeva et al., however, assigned the absorption peak at 1472 cm^{-1} to the chain mode CO adspecies.[7] In our calculations, we did not find CO adsorbed linearly on a low-coordinated O site. On the basis of our calculated values, it seems reasonable to attribute the two absorption peaks at 1475 and 1315 cm^{-1} to the chain-mode CO adsorbed on the low-coordinate O_{YC} (Y = 3,4) sites, and the species on O_{4C} site has higher C−O stretch frequency than does the species on O_{3C} site. This is reasonable, as the O_{3C} anion is known to have higher basicity and polarizability than does the O_{4C} anion and hence is easier to donate its electronic charge to the $2\pi^*$ MO of the adsorbed CO. For the C−O_{YC} stretch mode and O−C−O_{YC} (Y = 3,4) bend mode, no experimental value

TABLE 3: Calculated IR Frequencies[a] of CO_2^{2-} Surface Species (cm^{-1})

		free CO		$CO/(MgO)_4$		$CO/(MgO)_6$		CO/MgO
		B3LYP	expt.	nonrelax.	relax.	nonrelax.	relax.	expt.
ν_1	C−O stretch.	2204(2145)	2143	1455(1419)	1419(1383)	1533(1495)	1536(1498)	1475, 1315, 1280[b]
ν_2	$O-C-O_{XC}$ bend			726	737	836	800	850, 890[c]
ν_3	O_{XC}-C stretch			420(410)	798(778)	493(481)	962(938)	717, 743[c]

[a] Scale values for the C−O stretch mode are given in parentheses. [b] Refs 2 and 8. [c] Experimental values for the CO/CaO system extracted from ref 7.

TABLE 4: Calculated Vibrational Frequencies[a] of $C_2O_3^{2-}$ Species Formed on O_{4C} Site of the $(MgO)_6$ Cluster Model and of Triplet *trans*-$C_2O_3^{2-}$ Species Formed on O_{3C} Site of the $(MgO)_4$ Cluster Model and the IR Experimental Values for K_2 Species[b] in CO/MgO System

		$(CO)_2/(MgO)_4$		$(CO)_2/(MgO)_6$				
		triplet *trans*-$C_2O_3^{2-}$		singlet $C_2O_3^{2-}$	triplet *cis*-$C_2O_3^{2-}$	triplet *trans*-$C_2O_3^{2-}$		K_2 species[b]
	mode	nonrelax	relax	nonrelax	nonrelax	nonrelax	relax[d]	in CO/MgO
ν_1	C_2-O_2 str.	1731(1688)	1734(1691)	1645(1603)	1755(1711)	1707(1664)	1691(1650)	1615−1571
ν_2	C_1-O_1 str.	1488(1451)	1473(1436)	1569(1530)	1509(1471)	1508(1471)	1507(1470)	1473
ν_3	C_1-C_2 str.	1146	1175	C	1138	1167	1209	1180

[a] Only frequencies higher than 1000 cm^{-1} are given here. Scaled (scale factor 0.975) values are given in parentheses. [b] See ref 8. [c] The calculated value is 929 cm^{-1}. [d] The O_{YC} site is allowed to relax.

has been reported for the CO/MgO system, but for the CO/CaO system.[7] For comparison, we included these values in Table 3. The predicted frequencies of the $O_{YC}-C$ stretch mode and $O-C-O_{YC}$ ($Y = 3,4$) bend mode are lower than the corresponding experimental values,[7] probably due to the approximation that the O_{XC} site was fixed in the vibrational analysis. To show the effects of such an approximation, we tentatively relaxed the adsorptive O_{YC} sites in the $(MgO)_n$ ($n = 4,6$) clusters in the frequency calculations. The frequencies obtained are then 1498 (1383), 938(778), and 800(737) cm^{-1} for the C−O stretch, $C-O_{YC}$ stretch, and $O-C-O_{YC}$ bend modes for CO adsorbed on O_{4C} (O_{3C}), respectively, fitting better to the experimental values.

The vibrational frequencies of singlet dioxoketene ion $C_2O_3^{2-}$ formed at the O_{3C} site on $(MgO)_4$ has been calculated. Three highest frequencies are 2172 cm^{-1} (unscaled)/2118 cm^{-1} (scaled) for the O═C═C antisymmetrical stretching vibration, 1415 cm^{-1} (unscaled)/1380 cm^{-1} (scaled) for the O═C═C symmetrical stretching vibration, and 1096 cm^{-1} (unscaled)/1069 cm^{-1} (scaled) for the C−O stretching vibration. These values are comparable to the experimental data (2109−2084 cm^{-1}, 1378−1355 cm^{-1}, 1166 cm^{-1}) extracted from the IR spectra of CO/MgO by Babaeva et al.,[7] which were attributed to the ketenic $C_2O_3^{2-}$. However, the calculated formation energy of this dioxoketene anion is too low to convince us it is a stable surface species. We will show in a following paragraph that it is better to ascribe those absorption bands to the $C_3O_4^{2-}$ moiety, which also has a ketenic group and has substantial stability, rather than the singlet dioxoketene ion $C_2O_3^{2-}$ formed at the O_{3C} site, as suggested by Zecchina et al.[2] and Tashiro et al.[8]

The vibrational frequencies of singlet $C_2O_3^{2-}$, triplet *cis*-$C_2O_3^{2-}$, and triplet *trans*-$C_2O_3^{2-}$ species formed on the O_{4C} site of $(MgO)_6$ and of triplet *trans*-$C_2O_3^{2-}$ species formed on the O_{3C} site of $(MgO)_4$ have been calculated. The normal modes that have frequencies higher than 1000 cm^{-1} are listed in Table 4, together with the IR experimental values assigned to the K_2 species reported by Tashiro et al.[8] Originally we suspected that the K_2 species might be the dimeric, triplet *trans*-$C_2O_3^{2-}$ species, despite that Tashiro et al.[8] proposed the K_2 species was a chained tetramer on O^{2-} site. However, We see that the calculated values for the triplet *trans*-$C_2O_3^{2-}$ are in only rough agreement with the experimental values of K_2 species, even in the case that the adsorptive O_{YC} site is allowed to relax (see Table 4). Hence, it seems questionable to assign K_2 species to the dimeric adspecies. Considering the biradical nature and predicted low formation energy of the triplet $C_2O_3^{2-}$, we postulate that the K_2 species could be probably higher oligomers formed from the $C_2O_3^{2-}$ intermediate, e.g., the $C_4O_5^{2-}$ species proposed by Tashiro et al.,[8] the $C_{2n}O_{(2n+1)}^{2-}$ ($n \geq 3$) or $C_nO_{(n+2)}^{4-}$ ($n \geq 7$) species proposed by Zecchina et al.[2]

The calculated vibrational frequencies (>1000 cm^{-1}) of $C_3O_4^{2-}$ moiety formed on the O_{4C} site of $(MgO)_6$ model cluster are 2124, 1531, 1334, 1325, and 1007 cm^{-1} (scaled values). Taking the relaxation of the adsorptive O_{4C} site into account, we have correspondingly the values of 2122, 1542, 1335, 1343, and 1115 cm^{-1} (scaled values). Hence, allowing the relaxation of the adsorptive O_{YC} site improves significantly the theoretical prediction of the $C1-O_{4C}$ stretch frequency, but has negligible effect on the other vibrational modes of the $C_3O_4^{2-}$ moiety. In their IR study of the CO/MgO system, Tashiro et al. assigned the following five peaks at 2106−2091, 1570−1540, 1377−1350, 1320, and 1169−1155 cm^{-1} to K_3 species, and inferred that the K_3 species be in the $C_3O_4^{2-}$ form.[8] In their revised explanation of their TPD and IR experimental observations,[2] Zecchina et al. also proposed the presence of $C_3O_4^{2-}$ species in the CO/MgO chemisorption system. These inferences have been confirmed by our density functional cluster model calculations.

8. Concluding Remarks

The adsorption and adsorption-induced dimerization and trimerization of CO over the low-coordinated anionic sites of MgO solid have been investigated by means of the hybrid density functional B3LYP method in combination with the cluster model approach. The formation of anionic surface species, $C_mO_{m+1}^{2-}$ ($m = 1-3$), has been revealed to occur over those anionic surface sites of strong basicity. For the formation of $C_2O_3^{2-}$ surface species, it has been found that singlet dioxoketene ion $C_2O_3^{2-}$ can be formed at the O_{3C} site, while at the O_{4C} site the formation of triplet *trans*-$C_2O_3^{2-}$ is favorable over the formation of singlet $C_2O_3^{2-}$ species which has a long C−C bond length. The calculated energetics and electronic structures imply that either the singlet dioxoketene ion $C_2O_3^{2-}$ formed at the O_{3C} site or the triplet $C_2O_3^{2-}$ moiety formed at the O_{4C} site is intermediate-like and probably works as inter-

mediates leading to the formation of higher oligomers of CO. We also found that $C_3O_4^{2-}$ surface species having a ketenic O═C═C< group can be formed with substantial stability at O_{YC} ($Y = 3,4$) sites. The agreement between the calculated vibrational frequencies of these $C_mO_{m+1}^{2-}$ ($m = 1,3$) surface species and the experimental IR spectra of CO/MgO system is fairly good. Particularly, it should be mentioned that both $C_2O_3^{2-}$ and $C_3O_4^{2-}$ species may undergo further oligomerization with the formation of $C_mO_{m+2}^{4-}$ ($m \geq 6$) surface species. Further theoretical work is necessary to confirm such a possibility.

It is rather intriguing that CO adsorption over strongly basic sites of simple metal oxides gives rise to a variety of adspecies with rather complex IR spectra at low temperature and at room temperature. The special phenomena raise the possibility of utilizing CO, which is a widely used probe molecule for acidic sites in surface science, to probe the basicity of the surface sites on metal oxides at room or even higher temperatures. For this purpose, a better understanding of the inherent relationship between the basicity of the surface sites and the IR spectroscopic behavior of $C_mO_{m+1}^{2-}$ ($m = 1-3$) surface species is essential. This forms a meaningful subject of our future research.

Acknowledgment. This work was supported by the National Natural Science Foundation of China, the State Educational Commission of China, and Fok Ying Tung Education Foundation.

References and Notes

(1) Platero, E. E.; Scarano, D.; Spoto G.; Zecchina, A. *Faraday Discuss. Chem. Soc*. **1985**, *86*, 183.
(2) Zecchina, A.; Coluccia, S.; Spoto, G.; Scarano, D.; Marchese, L. *J. Chem. Soc., Faraday Trans.* **1990**, *86*, 703.
(3) Coluccia, S.; Baricco, M.; Marchese, L.; Martra, G.; Zecchina, A. *Spectrochim. Acta A* **1993**, *49*, 1289.
(4) Marchese, L.; Coluccia, S.; Martra, G.; Zecchina, A. *Surf. Sci.* **1992**, *269/270*, 135.
(5) Garrone, E.; Zecchina, A.; Stone, F. S. *J. Chem. Soc., Faraday Trans. 1* **1988**, *84*, 2843.
(6) Zecchina, A.; Scarano, D.; Bordiga, S.; Ricchiardi, G.; Spoto, G.; Geobaldo, F. *Catal. Today* **1996**, *27*, 403.
(7) Babaeva, M. A.; Bystrov, D. S.; Yu, A.; Tsygannenko, A. A. *J. Catal*. **1990**, *123*, 396.
(8) Tashiro, T.; Ito, J.; Sim, R. B.; Miyazawa, K.; Hamada, E.; Toi, K.; Kobayashi, H.; Ito, T. *J. Phys. Chem.* **1995**, *99*, 6115.
(9) Paukshtis, E. A.; Soltanov, R. I.; Yurchenko, N. E. *React. Kinet. Catal. Lett*. **1981**, *16*, 93.
(10) Furuyama, S.; Fujii, H.; Kawamura, M.; Morimoto, T. *J. Phys. Chem*. **1978**, *82*, 1028.
(11) Henry, C. R.; Chapon, C.; Duriez, C. *J. Chem. Phys*. **1991**, *95*, 700.
(12) He, J. W.; Estrada, C. A.; Corneille, J. S.; Wu, M. C.; Goodman, D. W. *Surf. Sci*. **1992**, *261*, 164.
(13) Morris, R. M.; Kaba, R. A.; Groshen, T. G.; Klaubunde, K. J.; Baltisberger, R. J.; Woolsey, N. F.; Stenberg, V. T. *J. Am. Chem. Soc*. **1980**, *102*, 3420.
(14) Morris, R. M.; Klabunde, K. J. *J. Am. Chem. Soc*. **1983**, *105*, 2633.
(15) Coluccia, S.; Marchese, L. *Catal. Today* **1998**, *41*, 229.
(16) Colbourn, E. A.; Mackrodt, W. C. *Surf. Sci*. **1982**, *117*, 571.
(17) Dovesi, R.; Orlando, R.; Ricca, F.; Roetti, C. *Surf. Sci*. **1987**, *186*, 267.
(18) Pacchioni, G.; Minerva, T.; Bagus, P. S. *Surf. Sci*. **1992**, *275*, 450.
(19) Neyman, K. M.; Ruzankin, S. Ph.; Rösch, N. *Chem. Phys. Lett*. **1995**, *246*, 546.
(20) Nygren, M. A.; Pettersson, L. G. M. *J. Chem. Phys*. **1996**, *105*, 9339, and references therein.
(21) Pelmenschikov, A. G.; Morosi, G.; Gamba, A.; Coluccia, S. *J. Phys. Chem. B* **1998**, *102*, 2226.
(22) Xu, X.; Nakatsuji, H.; Lu, X.; Ehara, M.; Cai, Y.; Wang, N.; Zhang, Q. *Theor. Chem. Acc.* **1999**, *102*, 170.
(23) Chen, L.; Wu, R.; Kioussis, N.; Zhang, Q. *Chem. Phys. Lett*. **1998**, *290*, 255.
(24) Snyder, J. A.; Alfonso, D. R.; Jaffe, J. E.; Lin, Z.; Hess, A. C.; Gutowski, M. *J. Phys. Chem. B* **2000**, *104*, 4717, and references therein.
(25) Matsumura, K.; Yamabe, S.; Fujioka, H.; Yanagisawa, Y.; Huzimura, R. *Phys. Rev. B* **1987**, *36*, 6145.
(26) Huzimura, R.; Yanagisawa, Y.; Matsumura, K.; Yamabe, S. *Phys. Rev. B* **1990**, *41*, 3786.
(27) Utamapanya, S.; Ortiz, J. V.; Klabunde, K. J. *J. Am. Chem. Soc*. **1989**, *111*, 799.
(28) Kobayashi, H.; Salahub, D. R.; Ito, T. *Catal. Today* **1995**, *23*, 357.
(29) Coluccia, S.; Garrone, E.; Guglielminotti, E.; Zecchina, A. *J. Chem. Soc., Faraday Trans. 1* **1981**, *77*, 1063.
(30) Wyckoff, R. W. G. *Crystal Structures*; Wiley: New York, 1963.
(31) Lu, X.; Xu, X.; Wang, N.; Zhang, Q.; Ehara, M.; Nakatsuji, H. *Chem. Phys. Lett.* **1998**, *291*, 109.
(32) Lu, X.; Xu, X.; Wang, N.; Zhang, Q. *Int. J. Quantum Chem*. **1999**, *73*, 377.
(33) Hass, K. C.; Schneider W. F.; Curioni, A.; Andreoni, W. *J. Phys. Chem. B* **2000**, *104*, 5527.
(34) Becke, A. D. *J. Chem. Phys*. **1993**, *98*, 5648.
(35) Lee, C.; Yang, W.; Parr, R. G. *Phys. Rev. B* **1988**, *37*, 785.
(36) Lu, X.; Xu, X.; Wang, N.; Zhang, Q. *J. Phys. Chem. B* **1999**, *103*, 3373.
(37) Lu, X.; Xu, X.; Wang, N.; Zhang, Q. *Chem. Phys. Lett*. **1999**, *300*, 109.
(38) Yanagisawa, Y.; Kuramoto, K.; Yamabe, S. *J. Phys. Chem. B* **1999**, *103*, 11078.
(39) Nicholas, J. B.; Kheir, A. A.; Xu, T.; Krawietz, T. R.; Haw, J. F. *J. Am. Chem. Soc*. **1998**, *120*, 10471.
(40) Sawabe, K.; Koga, N.; Morokuma, K.; Iwasawa, Y. *J. Chem. Phys*. **1994**, *101*, 4819.
(41) Frisch, M. J.; Trucks, G. W.; Schlegel, H. B.; Gill, P. M. W.; Johnson, B. G.; Robb, M. A.; Cheeseman, J. R.; Keith, T.; Petersson, G. A.; Montgomery, J. A.; Raghavachari, K.; Al-Laham, M. A.; Zakrzewski, V. G.; Ortiz, J. V.; Foresman, J. B.; Cioslowski, J.; Stefanov, B. B.; Nanayakkara, A.; Challacombe, M.; Peng, C. Y.; Ayala, P. Y.; Chen, W.; Wong, M. W.; Andres, J. L.; Replogle, E. S.; Gomperts, R.; Martin, R. L.; Fox, D. J.; Binkley, J. S.; Defrees, D. J.; Baker, J.; Stewart, J. P.; Head-Gordon, M.; Gonzalez, C.; Pople, J. A. *Gaussian 94*; Gaussian, Inc.: Pittsburgh, PA, 1995.
(42) Herzberg, G. *Electronic Spectra of Polyatomic Molecules*; Van Nostrand Reinhold: New York, 1966.
(43) Carpenter, J. E.; Weinhold, F. *J. Mol. Struct.—Theochem.* **1988**, *169*, 41.
(44) Lu, X.; Xu, X.; Wang, N.; Zhang, Q. *J. Phys. Chem. B* **1999**, *103*, 5657.